

Low-Temperature, High-Performance, Solution-Processed Indium Oxide Thin-Film Transistors

Seung-Yeol Han, Gregory S. Herman, and Chih-hung Chang*

School of Chemical, Biological and Environmental Engineering, Oregon State University, Corvallis, Oregon 97331, United States

S Supporting Information

ABSTRACT: Solution-processed In_2O_3 thin-film transistors (TFTs) were fabricated by a spin-coating process using a metal halide precursor, InCl_3 , dissolved in acetonitrile. A thin and uniform film can be controlled and formed by adding ethylene glycol. The synthesized In_2O_3 thin films were annealed at various temperatures ranging from 200 to 600 °C in air or in an O_2/O_3 atmospheric environment. The TFTs annealed at 500 °C under air exhibited a high field-effect mobility of $55.26 \text{ cm}^2 \text{ V}^{-1} \text{ s}^{-1}$ and an $I_{\text{on}}/I_{\text{off}}$ current ratio of 10^7 . In_2O_3 TFTs annealed under an O_2/O_3 atmosphere at temperatures from 200 to 300 °C exhibited excellent n-type transistor behaviors with field-effect mobilities of $0.85\text{--}22.14 \text{ cm}^2 \text{ V}^{-1} \text{ s}^{-1}$ and $I_{\text{on}}/I_{\text{off}}$ ratios of $10^5\text{--}10^6$. The annealing atmosphere of O_2/O_3 elevates solution-processed In_2O_3 TFTs to higher performance at lower processing temperature.

Transparent oxide semiconductors have been studied extensively as active layers in thin-film transistors (TFTs). Oxide-based semiconductors have performance advantages relative to hydrogenated amorphous silicon and organic semiconductors.¹ However, most oxide TFTs are fabricated by vacuum deposition techniques such as pulsed laser deposition and radio-frequency magnetron sputtering. Recently, a great deal of effort has been devoted to the advancement of solution-processed oxide semiconductors.² In our previous work, we developed a general chemistry capable of forming high-mobility metal oxide materials as channel layers for TFTs.^{1d,2b,2c,2i} However, the reported process used a high-temperature annealing step. In order to fabricate solution-processed oxide TFTs on flexible polymeric substrates, it is desirable to reduce the process temperature and enable greater process flexibility due to the lower thermal budget.

Indium oxide exhibits a variety of electrical properties, including metallic, semiconducting, and insulating characteristics depending on stoichiometry and defects in the material. Indium oxide is an insulator in its stoichiometric form, In_2O_3 . However, it is an n-type semiconductor in the oxygen-deficient form $\text{In}_2\text{O}_{3-\delta}$. With increasing oxygen deficiency, it acquires metallic characteristics. Indium oxide has high optical transparency with wide band-gap values between 3.5 and 4 eV. Because of these properties, the electronic device characteristic of indium oxide can be tuned by controlling defects in the material, including oxygen vacancies and indium interstitials.

A variety of techniques have been used for the preparation of high-quality indium oxide thin films, including evaporation,³

sputtering,⁴ spray pyrolysis,⁵ atomic layer deposition (ALD),⁶ ion-assisted deposition (IAD),⁷ pulsed laser deposition (PLD),⁸ and plasma-enhanced chemical vapor deposition (PECVD).⁹ Recently, there have been efforts to fabricate transparent oxides via solution-based processes.² Lee et al.^{2b} reported a general and low-cost solution route for the fabrication of high-mobility metal oxide semiconductors. A variety of thin-film metal oxide semiconductors including binary compounds (ZnO , In_2O_3 , SnO_2 , Ga_2O_3), ternary compounds (ZIO, ITO, ZTO, IGO), and quaternary compounds (IZTO, IGZO) have been fabricated successfully using this route.¹⁰ Here we report a novel annealing strategy that results in high-performance TFTs using solution-processed In_2O_3 channel layers at lower temperatures. The effect of the annealing atmosphere on the In_2O_3 film's optical, morphological, chemical, and electrical properties as well as the TFT performance was studied. High-performance indium oxide TFTs were successfully fabricated at low temperatures (<250 °C).

The In_2O_3 precursor solution was prepared using InCl_3 and ethylene glycol (EG) in acetonitrile. InCl_3 was dissolved in acetonitrile at 0.05 M, and EG was subsequently added. We found that EG enhanced the formation of thin, uniform films. An EG/acetonitrile volume ratio of 1:50 was used in these studies. Both microscope glass slides and oxidized silicon substrates were used for fabricating In_2O_3 thin films. The synthesized In_2O_3 thin films were annealed at various temperatures from 200 to 600 °C under different atmospheric conditions, including air and O_2/O_3 . The In_2O_3 active layers were patterned to avoid fringing current artifacts. The detailed fabrication procedure for the indium oxide TFTs is illustrated in Figure 1 and described in the Supporting Information.

In_2O_3 thin films annealed in air or under an O_2/O_3 atmosphere were amorphous as determined by X-ray diffraction (XRD), similar to other oxide semiconductors fabricated using the same route.^{2e,f} The spin-coated In_2O_3 thin films showed very uniform morphologies, with an average roughness of $0.27 \pm 0.04 \text{ nm}$ as measured by tapping-mode atomic force microscopy (AFM) (Figure S1 in the Supporting Information). They were highly transparent in the visible wavelength range with a transmittance larger than 98%; optical band gap and transmittance data for films annealed under different atmospheres at temperatures are shown in Figure S2. The band-gap values for films annealed in O_2/O_3 (3.5–3.7 eV) were found to be slightly lower than the values for films annealed in air (3.7–3.85 eV). X-ray photoelectron spectroscopy (XPS) O 1s spectra (Figure 2a) could be deconvoluted into two peaks, one located at 530.6 eV

Received: June 16, 2010

Published: March 18, 2011

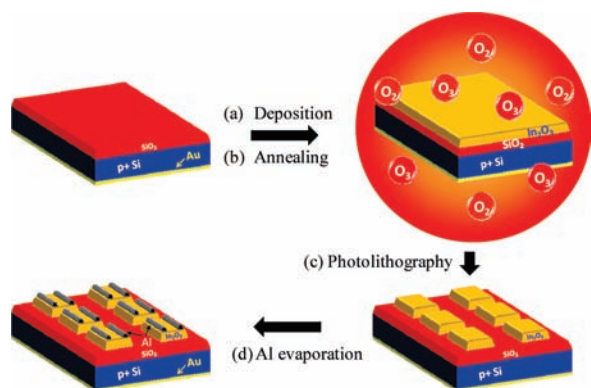


Figure 1. Schematic illustration of the fabrication of TFT devices: (a) film deposition by a spin-coating process; (b) annealing under different atmospheric conditions; (c) patterning of the photoresist layer and etching of the In_2O_3 thin film; (d) deposition of source and drain electrodes by Al evaporation.

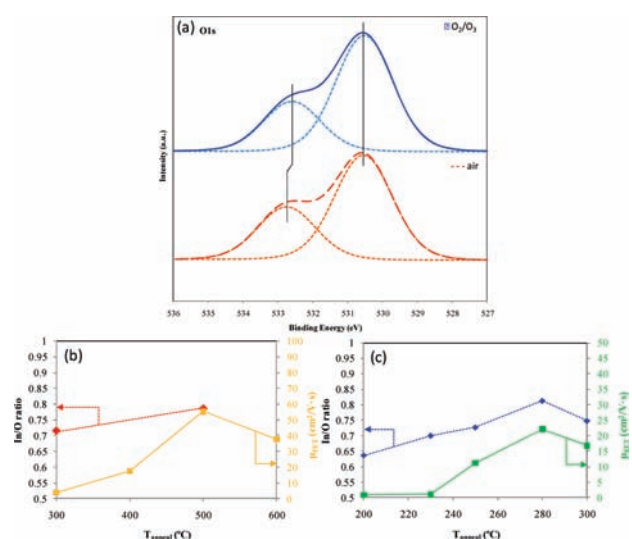


Figure 2. (a) O 1s XPS spectra of the In_2O_3 thin films annealed in air and an O_2/O_3 environment at $300\text{ }^\circ\text{C}$ for 2 h. The oxygen amounts at 530.6 eV for annealing in air and O_2/O_3 were 63.4 and 71.3 atom %, respectively, giving an air/ozone ratio of 0.889. (b, c) Total In/O atomic ratios and field-effect mobilities as functions of annealing temperature (b) in air and (c) in an O_2/O_3 atmosphere. The In/O atomic ratio was ~ 0.8 at the highest point, which presents the lowest oxygen ratio and indicates the highest mobility under both sets of atmospheric conditions).

and the other at ~ 532.8 eV. Prior studies of In_2O_3 suggested that the peak at 530.6 eV corresponds to O^{2-} ions with neighboring indium atoms having their full complement of six nearest-neighbor O^{2-} .^{11,12} The peak at higher binding energies near 533 eV corresponds to O^{2-} at an oxygen-deficient indium site or to a hydroxyl group.^{11,12} The In/O atomic ratios of films annealed in air and ozone at $300\text{ }^\circ\text{C}$ were investigated, and the results are shown in Table S1 in the Supporting Information. Comparison of the ratio of the O 1s peaks at 530.6 eV for films annealed in ozone and air indicated that the films annealed in ozone have more oxygen with such binding. In contrast, films annealed in ozone have larger total In/O ratios than those annealed in air, as shown in Table S1 and Figure 2b,c. An O 1s peak shift at binding energy

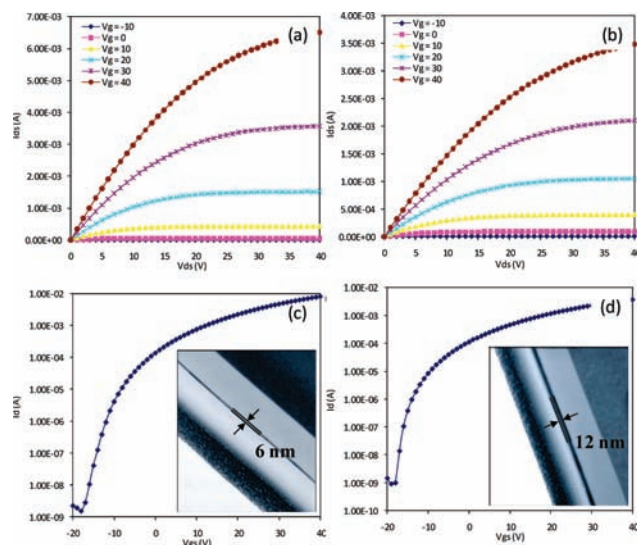


Figure 3. (a, b) Output and (c, d) transfer characteristics of In_2O_3 TFTs for devices annealed (a, c) at $500\text{ }^\circ\text{C}$ under air and (b, d) at $280\text{ }^\circ\text{C}$ under O_2/O_3 . The insets in (c) and (d) show TEM cross-sectional images of films annealed under each set of conditions.

near 533 eV was found for comparing films annealed in air and ozone (Figure 2a). The O 1s peak of films annealed in ozone at 533 eV indicates that these films contain more oxygen-deficient sites than films annealed in air, which have more hydroxyl groups and fewer oxygen-deficient sites. The XPS results suggest that the films annealed in O_2/O_3 contain more fully coordinated indium sites with six nearest-neighbor oxygens and more oxygen-deficient sites, and the air-annealed films contain less fully coordinated indium sites and more hydroxyl groups. Figure 2b, c also shows that the highest-mobility TFTs have an In/O atomic ratio of ~ 0.8 under both sets of annealing conditions, indicating that ozone annealing leads to lower processing temperatures with high performance in TFT fabrication. This is a very interesting finding, but it is not yet fully proven.

The TFT performance was characterized in an ambient environment. Shown in Figure 2b,c are the resulting field-effect mobilities for devices annealed under different atmospheric conditions and temperatures of the TFT with a patterned In_2O_3 active layer. The indium oxide TFTs show good gate-modulated transistor characteristics for films annealed in air for temperatures between 300 and $600\text{ }^\circ\text{C}$. The highest mobility of $55.26\text{ cm}^2\text{ V}^{-1}\text{ s}^{-1}$ along with an excellent $I_{\text{on}}/I_{\text{off}}$ current ratio of 10^7 , was achieved for indium oxide films annealed in air at $500\text{ }^\circ\text{C}$, as shown in Figures 2b and 3a,c. The TFTs fabricated from In_2O_3 films annealed in oxygen-rich atmosphere (i.e., O_2/O_3) also demonstrated excellent output and transfer characteristics, with a high mobility of $22.14\text{ cm}^2\text{ V}^{-1}\text{ s}^{-1}$ along with an excellent $I_{\text{on}}/I_{\text{off}}$ ratio of 10^6 , as shown in Figures 2c and 3b,d. The thickness of films annealed under different atmospheric conditions at various temperatures was investigated by cross-sectional transmission electron microscopy (TEM), and TEM images are given as insets in Figure 3c,d. The observed difference in the thickness of these films is likely caused by the different annealing temperatures. The film annealed at a higher temperature (i.e., $500\text{ }^\circ\text{C}$) is thinner than the film annealed at a lower temperature (i.e., $280\text{ }^\circ\text{C}$). We plan to perform additional physical and chemical characterizations to further understand the cause and

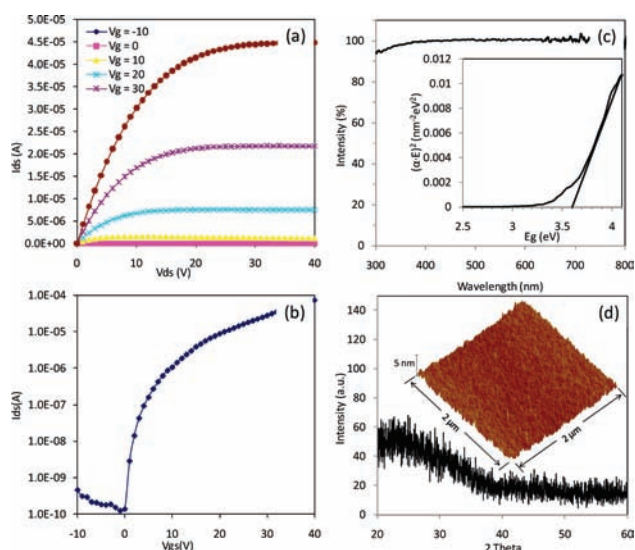


Figure 4. (a) Output and (b) transfer characteristics of solution-processed In_2O_3 TFTs. (c) Transmittance of an In_2O_3 thin film on a glass slide (inset: estimated band gap of the In_2O_3 thin film). (d) XRD pattern of an amorphous In_2O_3 thin film (inset: AFM image of the In_2O_3 thin film). All of the films were annealed in an O_2/O_3 environment at 230°C for 2 h.

nature of this difference. The corresponding device characteristics are summarized in Table S2 for $V_{\text{ds}} = 40\text{ V}$. A comparison of the device performance of In_2O_3 films annealed in air and O_2/O_3 at 300°C is presented in Figure S3. The TFTs fabricated from indium oxide thin films annealed under an O_2/O_3 atmosphere at temperatures lower than 300°C showed excellent n-type transistor behavior with a field-effect mobility as high as $22.14\text{ cm}^2\text{ V}^{-1}\text{ s}^{-1}$ and an $I_{\text{on}}/I_{\text{off}}$ ratio of 10^5 – 10^6 . The lowest processing temperature for indium oxide TFTs that showed reasonable field-effect properties ($\mu_{\text{FE}} = 0.85\text{ cm}^2\text{ V}^{-1}\text{ s}^{-1}$, $I_{\text{on}}/I_{\text{off}}$ ratio = 10^5) was achieved by annealing under an O_2/O_3 atmosphere at 200°C .

The output and transfer characteristics of an indium oxide TFT annealed in O_2/O_3 at 230°C are shown in Figure 4a,b. This low-temperature-fabricated indium oxide TFT had a mobility of $1.05\text{ cm}^2\text{ V}^{-1}\text{ s}^{-1}$, an $I_{\text{on}}/I_{\text{off}}$ ratio of 10^6 , and a positive V_{on} , which are well-suited for TFT LCDs (see Figure S4 for V_{on} as function of annealing temperature under air and O_2/O_3). Recently, Jeong et al.¹² reported the effect of oxygen deficiencies and the role of gallium in dramatically lowering the processing temperature for solution-derived indium zinc oxide TFTs. A field-effect mobility of $0.05\text{ cm}^2\text{ V}^{-1}\text{ s}^{-1}$ and $I_{\text{on}}/I_{\text{off}}$ ratio of 10^5 were achieved for IGZO TFTs at a processing temperature of 250°C .¹² Kim et al.^{2f} reported high-performance solution-processed indium oxide TFTs for which a field-effect mobility of up to $0.7\text{ cm}^2\text{ V}^{-1}\text{ s}^{-1}$ and an $I_{\text{on}}/I_{\text{off}}$ ratio of 10^6 were achieved using a combination of solution-processed intrinsic In_2O_3 (400°C air annealing) and SiO_2 as a gate dielectric layer. In contrast, a field-effect mobility of up to $43.7\text{ cm}^2\text{ V}^{-1}\text{ s}^{-1}$ and an $I_{\text{on}}/I_{\text{off}}$ ratio of 10^6 were achieved when high- k organic nanodielectrics were used as a gate dielectric layer. These results suggest that further improvements in TFT performance can be achieved for these low-temperature solution-processed indium oxide thin films by optimizing the semiconductor/dielectric layers and interfaces.

In conclusion, high-performance solution-processed indium oxide TFTs were successfully fabricated. Field-effect mobilities as

high as $55.26\text{ cm}^2\text{ V}^{-1}\text{ s}^{-1}$ were achieved, which is significantly higher than those for other solution-processed semiconductors and even higher than previously reported vacuum-processed indium oxide TFTs using SiO_2 as a gate dielectric layer.^{7,9} More importantly, TFTs fabricated from In_2O_3 films annealed at lower temperatures ($<250^\circ\text{C}$) under an oxygen-rich atmosphere (i.e., O_2/O_3) also showed good output and transfer characteristics. This work demonstrates a general low-temperature solution route for fabrication of transparent oxide TFTs.

■ ASSOCIATED CONTENT

S Supporting Information. Detailed procedure of film deposition for TFT fabrication and results of characterizations. This material is available free of charge via the Internet at <http://pubs.acs.org>.

■ AUTHOR INFORMATION

Corresponding Author

changch@che.orst.edu

■ ACKNOWLEDGMENT

C.-H.C. acknowledges support from a National Science Foundation CAREER Grant (CTS-0348723) and the Sharp Laboratories Scholar Fund.

■ REFERENCES

- (1) (a) Nomura, K.; Ohta, H.; Takagi, A.; Kamiya, T.; Hirano, M.; Hosono, H. *Nature* **2004**, *432*, 488. (b) Fortunato, E. M. C.; Barquinha, P. M. C.; Pimentel, A.; Goncalves, A.; Marques, A.; Pereira, L.; Martins, R. *Adv. Mater.* **2005**, *17*, 590. (c) Hsieh, H.-H.; Wu, C.-C. *Appl. Phys. Lett.* **2007**, *91*, No. 013502. (d) Han, S.-Y.; Lee, D.-H.; Herman, G. S.; Chang, C.-H. *J. Disp. Technol.* **2009**, *5*, 520.
- (2) (a) Sun, B.; Peterson, R. L.; Sirringhaus, H.; Mori, K. *J. Phys. Chem. C* **2007**, *111*, 18831. (b) Lee, D.-H.; Chang, Y.-J.; Herman, G. S.; Chang, C.-H. *Adv. Mater.* **2007**, *19*, 843. (c) Chang, Y.-J.; Lee, D.-H.; Herman, G. S.; Chang, C.-H. *Electrochem. Solid-State Lett.* **2007**, *10*, H135. (d) Cheng, H. C.; Chen, C. F.; Tsay, C. Y. *Appl. Phys. Lett.* **2007**, *90*, No. 012113. (e) Choi, C. G.; Seo, S.-J.; Bae, B.-S. *Electrochem. Solid-State Lett.* **2008**, *11*, H7. (f) Kim, H. S.; Byrne, P. D.; Facchetti, A.; Marks, T. J. *J. Am. Chem. Soc.* **2008**, *130*, 12580. (g) Meyers, S. T.; Anderson, J. T.; Hung, C. M.; Thompson, J.; Wager, J. F.; Keszler, D. A. *J. Am. Chem. Soc.* **2008**, *130*, 17603. (h) Li, C.-S.; Li, Y.-N.; Wu, Y.-L.; Ong, B.-S.; Loutfy, R.-O. *J. Mater. Chem.* **2009**, *19*, 1626. (i) Lee, D.-H.; Han, S.-Y.; Herman, G. S.; Chang, C.-H. *J. Mater. Chem.* **2009**, *19*, 3135.
- (3) (a) Naseem, S.; Rauf, I. A.; Hussain, K.; Malik, N. A. *Thin Solid Films* **1988**, *156*, 161. (b) Dhananjay, Chu, C.-W. *Appl. Phys. Lett.* **2007**, *91*, No. 132111.
- (4) (a) Bellingham, J. R.; Phillips, W. A.; Adkins, C. J. *J. Phys.: Condens. Matter.* **1990**, *2*, 6207. (b) Bender, M.; Katsarakis, N.; Gagaoudakis, E.; Hourdakis, E.; Douloufakis, E.; Cimalla, V.; Kiriakidis, G. *J. Appl. Phys.* **2001**, *90*, 5382.
- (5) (a) Manoy, P. K.; Gopchandran, K. G.; Joseph, B.; Koshy, P.; Vaidyan, V. K. *Indian J. Phys.* **2001**, *75A*, S07. (b) Manoy, P. K.; Gopchandran, K. G.; Koshy, P.; Vaidyan, V. K.; Joseph, B. *Opt. Mater.* **2006**, *28*, 1405.
- (6) Nilsen, O.; Balasundaraprabhu, R.; Monakhov, E. V.; Muthukumarasamy, N.; Fjellvåg, H.; Svensson, B. G. *Thin Solid Films* **2009**, *517*, 6320.
- (7) (a) Wang, L.; Yoon, M.-H.; Lu, G.; Yang, Y.; Facchetti, A.; Marks, T. J. *Nat. Mater.* **2006**, *5*, 893. (b) Wang, L.; Yoon, M.-H.; Facchetti, A.; Marks, T. J. *Adv. Mater.* **2007**, *19*, 3252.

(8) Adurodija, F. O.; Izumi, H.; Ishihara, T.; Yoshioka, H.; Matusi, H.; Motoyama, M. *Appl. Phys. Lett.* **1999**, *74*, 3059.

(9) Vygranenko, Y.; Wang, K.; Nathan, A. *Appl. Phys. Lett.* **2007**, *91*, No. 263508.

(10) (a) Park, S. K.; Kim, Y.-H.; Kim, H.-S.; Han, J.-I. *Electrochem. Solid-State Lett.* **2009**, *12*, H256. (b) Chen, C.-K.; Hsieh, H.-H.; Shyue, J.-J.; Wu, C.-C. *J. Disp. Technol.* **2009**, *5*, 509. (c) Lee, C.-G.; Dodabalapur, A. *Appl. Phys. Lett.* **2010**, *96*, No. 243501.

(11) (a) Wu, W.-F.; Chiou, B.-S. *Semicond. Sci. Technol.* **1996**, *11*, 196. (b) Fan, J. C. C.; Goodenough, J. B. *J. Appl. Phys.* **1977**, *48*, 3524. (c) Wu, W. F.; Chiou, B. S.; Hsieh, S. T. *Semicond. Sci. Technol.* **1994**, *9*, 1242.

(12) Jeong, S.; Ha, Y.-G.; Moon, J.; Facchetti, A.; Marks, T. J. *Adv. Mater.* **2010**, *22*, 1346.